Test Methodology for the Determination of Optimum Fusion Welding Conditions of Polyethylene

D. SAINT-ROYRE, D. GUEUGNAUT, and D. REVERET,
Direction des Etudes et Techniques Nouvelles du Gaz de France, Centre d'Etudes et de Recherches sur les Sciences et Techniques Appliquées, 361 Avenue du Président Wilson, 93210 La Plaine Saint-Denis, France

Synopsis

The fusion welding behavior of a medium density polyethylene resin has been studied for a wide range of heating rates using a recently developed test methodology. With this method, the thermal and physical phenomena occurring at the interface of two thin polyethylene pieces assembled by fusion can be studied. It consists of a thermal welding phase and a phase of mechanical separation of the welded assembly. For the mechanical phase, an adaptation of the T-peel test was used. These conditions make it possible to determine the thermal welding parameters (temperature, time) for optimal mechanical quality of the joint, according to a criterion established by optimization of the peel test used. The variations in minimum temperature required for an optimum weld, as a function of heating rate, can be simulated with a numerical model based on the concept of macromolecular interdiffusion. Consistent with the experimental behavior, the numerical model involves two parameters characteristic of the diffusion behavior of the polyethylene resin. Thus, these parameters characterize the weldability of the polyethylene resin under study.

INTRODUCTION

In order to determine the optimum conditions for fusion welding of bulk polyethylene pieces, two conditions must be satisfied. First, the physicochemical phenomena that occur during welding (responsible for the microscopic bonds in the material) and the kinetics of these phenomena must be understood. Then, the temperature at each point, and especially at the interface, must be known throughout the welding period.

Significant thermal gradients in the welded bulk pieces make the study difficult. It was therefore necessary to develop a specific test methodology in order to satisfy the first condition. It uses small-sized specimens. As the assembly is reduced to its interface, the welded plane can be perfectly characterized both thermally and mechanically.

This methodology consists of a thermal welding phase and a mechanical separation phase derived from a peel test. It was used to determine the conditions of temperature and time required to obtain optimal mechanical quality of the welded joint. The results obtained were interpreted using welding theories based on the concept of adhesion by macromolecular interdiffusion.

Journal of Applied Polymer Science, Vol. 38, 147–162 (1989)
 CCC 0021-8995/89/010147-16$04.00

TECHNIQUE AND EQUIPMENT

Methodology

The test methodology developed is used to study the phenomena relating to the welding and separation of polyethylene microspecimens [Fig. 1(A)]. It involves two consecutive phases. The first is a fusion welding phase under well-defined conditions of temperature and time [Fig. 1(B)]. The second is a separation phase of the welded joint by a peel test devised to take account of the material and the shape of specimens used [Fig. 1(C)]. The welding by fusion of two polyethylene specimens may be isothermic or dynamic. For practical reasons, the latter was chosen. Welding cycles, consisting of controlled heating and cooling, were carried out with different heating rates, as shown in Figure 2. In all cases, these cycles were symmetrical, i.e., the heating

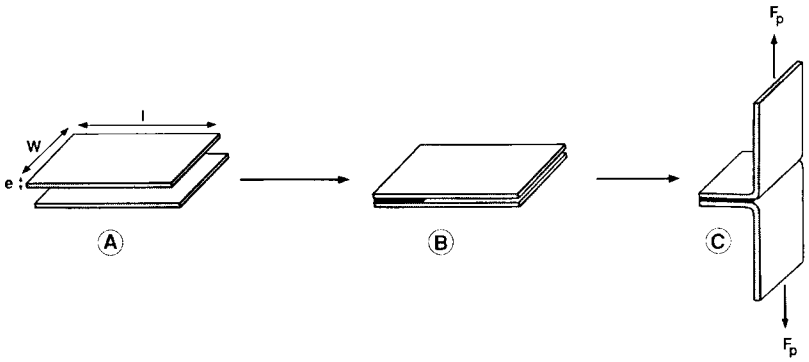

Fig. 1. Test methodology: (A) Geometry of polyethylene specimens: l = length, W = width, e = thickness of films. (B) Heating stage: the welded zone represents about 1/3 of the total area $l \times W$. (C) Mechanical separation phase: the test used is a T-peel test (at 180°), with constant load F_p.

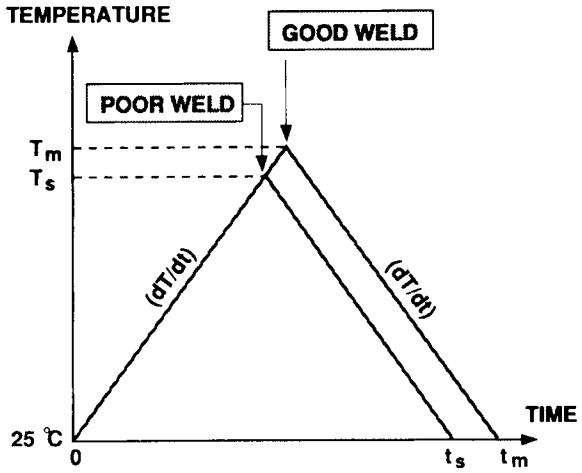

Fig. 2. Heating phase: The different cycles tested provide a definition of T_s, the temperature at the peak of the cycle, and t_s, the total duration of the cycle for the heating rate $[dT/dt]$. T_m represents the minimum temperature required to obtain a good weld and t_m the total duration of the corresponding cycle (total welding time).

and cooling rates were identical. As shown in Figure 2, each welding condition could be completely characterized according to two thermal parameters. The former was the programmed heating rate $[dT/dt]$, expressed in °C/min and the latter was temperature at the cycle peak, T_s. It was also possible to define a heating time $\frac{1}{2}t_s$, corresponding to the parameters ($[dT/dt]$; T_s).

The peel test was used to define a criterion relating to the quality of the welded joint. With this criterion, it was possible to determine T_m, the minimum temperature required for a "good weld" for each heating rate $[dT/dt]$. T_m is the lower limit temperature above which welding is optimal for the heating rate considered. The corresponding heating time is therefore equal to $\frac{1}{2}t_m$.

For a given heating rate, the lower limit T_m was reached step by step. For each $[dT/dt]$, a minimum of five temperatures graduated by steps of 5 or 10°C, was necessary to determine optimum theoretical conditions ($[dT/dt]$; T_m).

Experimental Setup for Fusion Welding Process

Heating Cell. With our experimental setup, fusion welds could be achieved over a very wide range of temperatures and heating rates. The range of rates between 20 and 400°C/min was studied in particular. The heating and cooling system was composed of three elements: a Micristar process controller (Model 828D Research Inc., Minneapolis, MN), a Servofram SRD (Sefram, Paris) "temperature–time" graphic recording unit, and a quad elliptical heating chamber (Model E4-2, Research Inc. Minneapolis) connected to a gaseous nitrogen cooling system. Heating was provided by infrared radiation with four tubular tungsten filament quartz lamps (Model Q1000 T3/4CL, Research Inc., Minneapolis) mounted in four elliptical reflectors. The radiation thus converged at the geometrical center of the cell where the samples to be welded were placed. The local temperature was measured with an insulated thermocouple (Model TC, 100 Gordon Company, Richmond, IL) connected to the process controller. The power required for heating was supplied by a phaser power controller (Model 64600, Research Inc., Minneapolis).

Sample Handling. A specific device has been developed to maintain the specimens to be welded in the center of the cell. It is presented in Figure 3(a). The dimensions of the specimens were kept invariable by means of a brass crucible, on the lid of which a known pressure was applied throughout the heating cycle. Welding pressure was obtained by the compression of two inconel springs specially treated for high temperature applications. Figure 3(b) shows the parts of this holding device and the positioning of the specimens. The mutual contact area between the two films to be assembled was 6×6 mm^2. It was defined by placing an aluminum separator 10 mm long and less than 0.05 mm thick between the two PE films. In order to apply even welding pressure, a thickness compensation was made by placing an identical but 6-mm-long aluminum plate between the upper specimen and the cell lid [see Fig. 3(b)]. The particular design of this device allowed one to record the temperature of the specimens continuously and to control perfectly the welding phase with a relative accuracy better than 4% on the heating and cooling rates. Under these conditions, the lower limits T_m were determined with an accuracy of about ± 2.5°C.

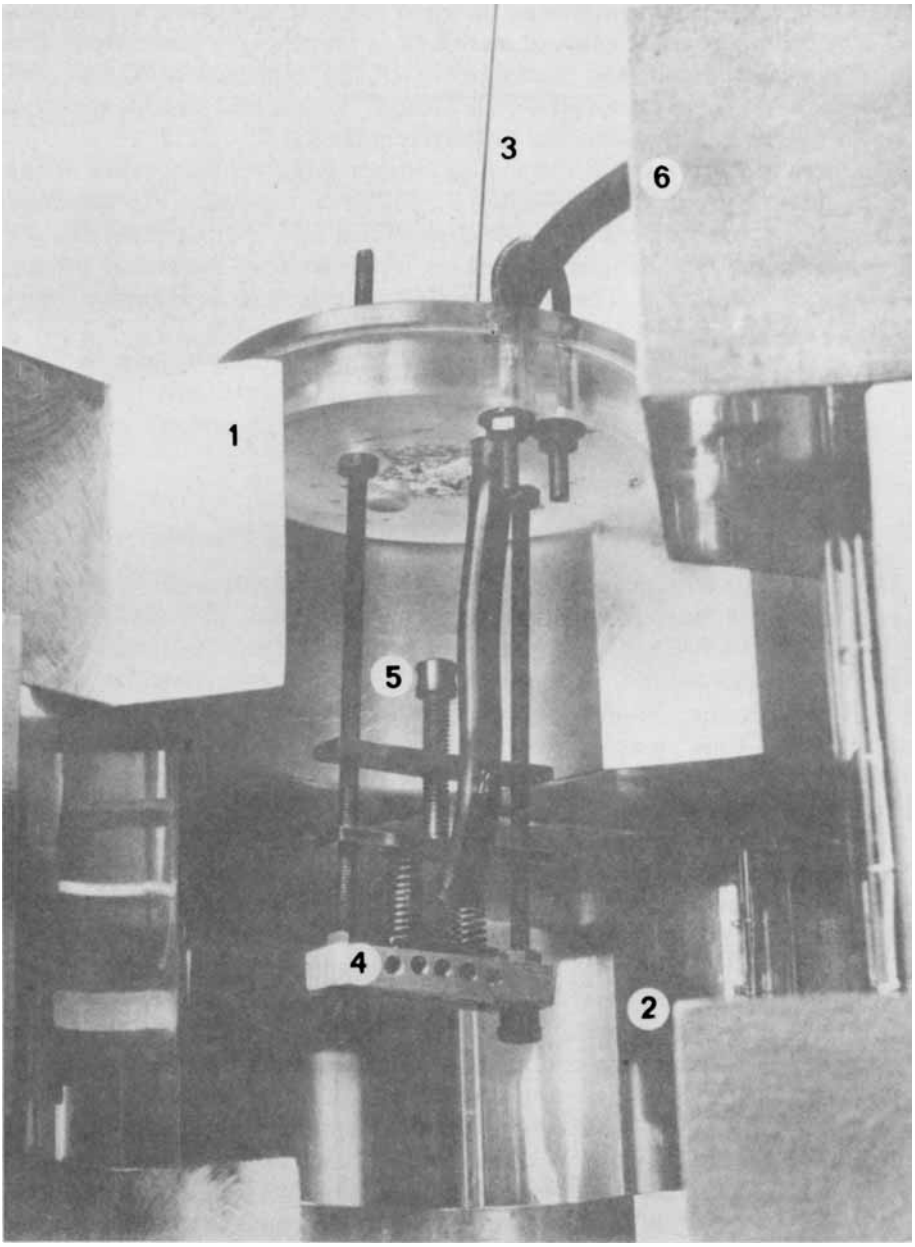

(a)

Fig. 3. Experimental device for holding the PE sheets to be welded: (a) Overall view: (1) base of cell; (2) tungsten filament lamp; (3) thermocouple; (4) holding device for crucible containing PE films; (5) device for exerting welding pressure; (6) cooling gas (nitrogen) inlet. (b) Diagram of the holding setup for PE sheets to be welded: (1) Thermocouple; (2) welding pressure; (3) compression springs; (4) brass crucible lid; (5) 6 mm aluminum plate (~ 50 μm thick) for thickness compensation; (5′) 10 mm aluminum plate; (6) PE specimens, length 16 mm, thickness 0.38 mm; (7) brass holding crucible; (8) contact area to be welded (6×6 mm^2).

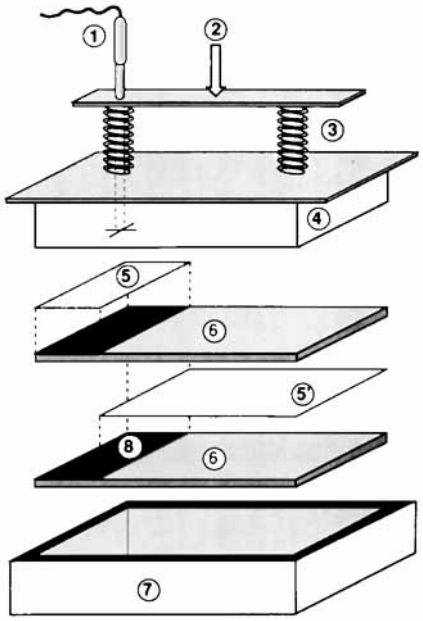

(b)

Fig. 3. (*Continued from the previous page.*)

Experimental Peeling Setup

Description. The principle of the T-peel test [see Fig. 1(C)] has been adapted for mechanical characterization of welded polyethylene microspecimens. The test is a highly effective means to examine the physicochemical phenomena at the interface of the two polymers.[1-4] Because of the specimen dimensions and the need to avoid creep or sudden breaking from overload, the constant load–peel tests are the most suitable.[4,5] Thus, the material is maintained near thermodynamic equilibrium throughout the test. Previous studies have revealed the influence of the environment in which the peeling is carried out.[1,4,5] In particular, temperature is an accelerating factor. For this reason, a temperature of 80°C was used. This corresponds approximately to the temperature at which melting starts in the semicrystalline polyethylene studied. The chosen conditions made it possible first to localize the crack at the interface. Secondly the problem of plastic deformation of the films was avoided and viscoelastic deformations were minimized thanks to low load application speeds.

The T-peel tests were achieved with a particular peeling device. The welded joints were pulled apart inside the oven of a thermomechanical analyzer (Model TMA40, Mettler Instr. AG-CH-8606 Greifensee, Switzerland) equipped with a quartz tensile system (Fig. 4). Load was applied to the joints after thermal stabilization in the oven of the TMA.

Data Processing. Using this peeling device, the elongation ($L - L_0$) of the welded joint vs. time and the corresponding instantaneous peel rate were recorded. A data processing program, developed on a Hewlett-Packard microcomputer (Model 9836) connected to the Mettler system, calculated the

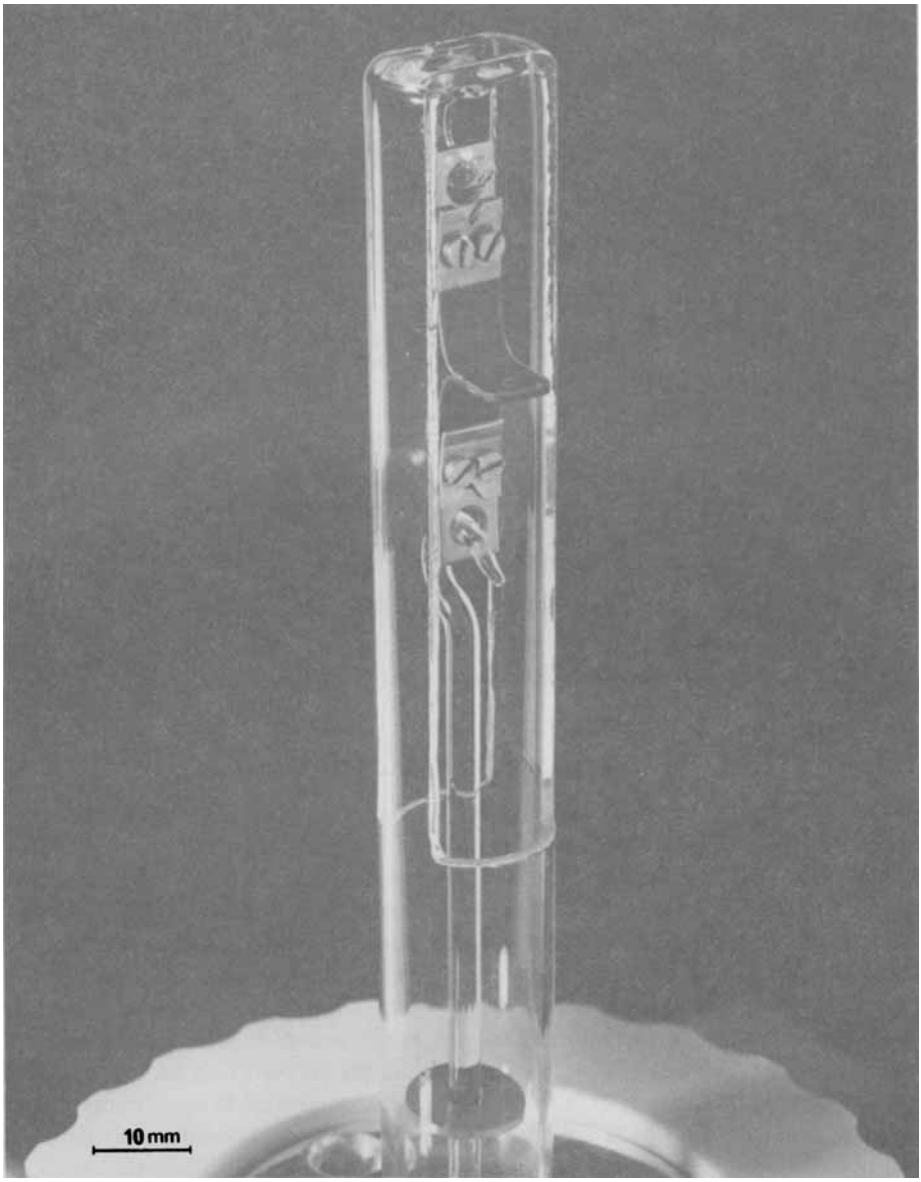

Fig. 4. Mechanical separation device: quartz microtensile device for T-peel test. A PE welded assembly can be seen at the top.

average peel rate $\overline{V}_p$, where

$$\overline{V}_p = \frac{\int (dL/dt) \cdot dL}{\int dL}$$

taking account of the phenomena related to temperature and load application to the joint at the beginning of the test.

Optimum Fusion Welding Criterion. In light of the considerations discussed above, it was necessary to optimize the experimental conditions. The

temperature of the TMA oven was set at 80°C and the load applied was 210 g, the maximum permitted value for the thermomechanical analyzer. The oven atmosphere was also controlled by flushing with nitrogen. Based on this optimization, a criterion representing the weld quality of the two polyethylene specimens was established. According to this criterion, the weld was considered to be good if the average peel rate $\bar{V}_p$ was close to 0 μm/min for a test duration of 1000 min. In practice, the viscoelasticity of the system, and a slight slipping of the material in the tensile clamps resulted in a mean rate $\bar{V}$ of about 0.1–0.2 μm/min. This range of values was substantially the same as a zero-peel rate. Optimum thermal welding conditions ($[dT/dt]$; T_m) were considered to be reached when the peel rate $\bar{V}_p$ was lower than or equal to $\bar{V}$ (Fig. 5).

Under these conditions, the energy of cohesion of the weld G was at least equal to

$$G_m = 2 \cdot F_p \cdot W \tag{1}$$

where F_p is the force applied during the peel test and W the width of the specimens[1,4] (see Fig. 5).

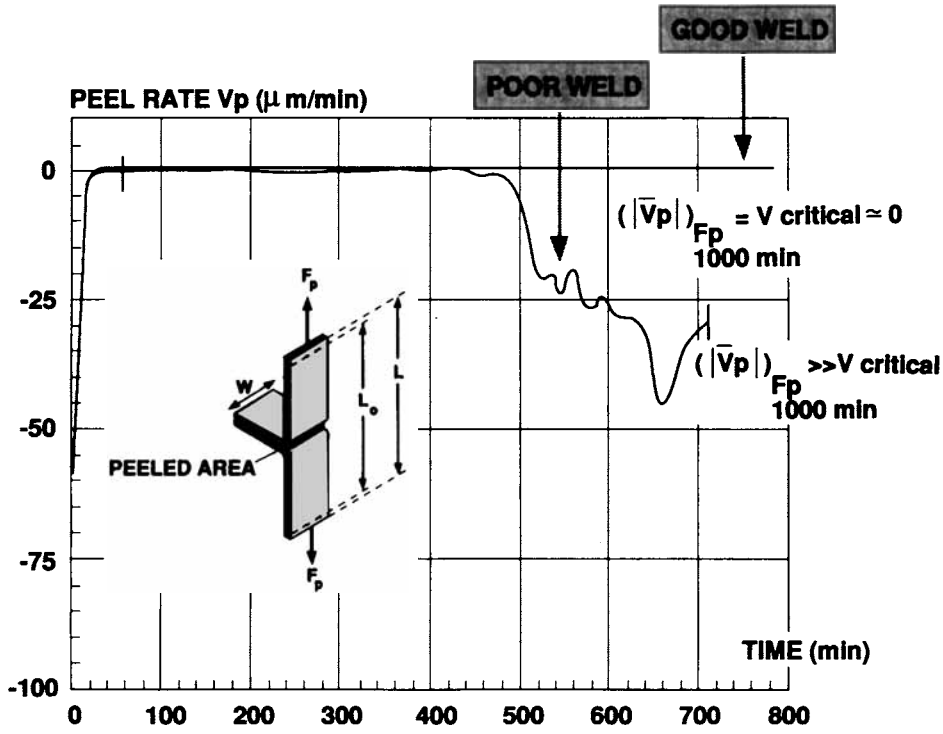

Fig. 5. Criterion of fusion welding quality: A good weld ($\bar{V}_p \sim 0$) corresponds to the given conditions ($[dT/dt]$; T_m). The vertical dashes on the curve define the limits between which the average peel rate $\bar{V}_p$ was calculated. V_{critical} is about 0.1–0.2 μm/min.

Samples Studied

The samples studied were taken from a pipe with external diameter 110 mm and thickness 10 mm, extruded from a commercial resin (BP Chemicals, Grangemouth, Stirlingshire, United Kingdom) (density ≈ 0.948 g cm^{-3}; $\overline{M}_w$ ~ 150,000; polydispersity about 9).

Films between 0.36 and 0.38 mm thick were microtomed from the midwall of a pipe. Thus, the surface orientation phenomena due to the pipe manufacturing process were avoided. The microspecimens were obtained from these films by cutting with a punch. The samples to be welded were in the form of thin rectangular sheets measuring 16 × 6 mm. Before welding, the samples were cleaned with methyl ethyl ketone.

RESULTS AND DISCUSSION

Experimental Fusion Welding Behavior of Polyethylene

Figure 6 shows the variations in minimum temperature T_m required to obtain a good weld as a function of the heating rate dT/dt.

For rates under about 150°C/min, T_m increases rapidly with dT/dt. For heating rates greater than 150°C/min, T_m varies rather linearly with dT/dt. For the entire range studied, the variation of T_m vs. dT/dt can be described

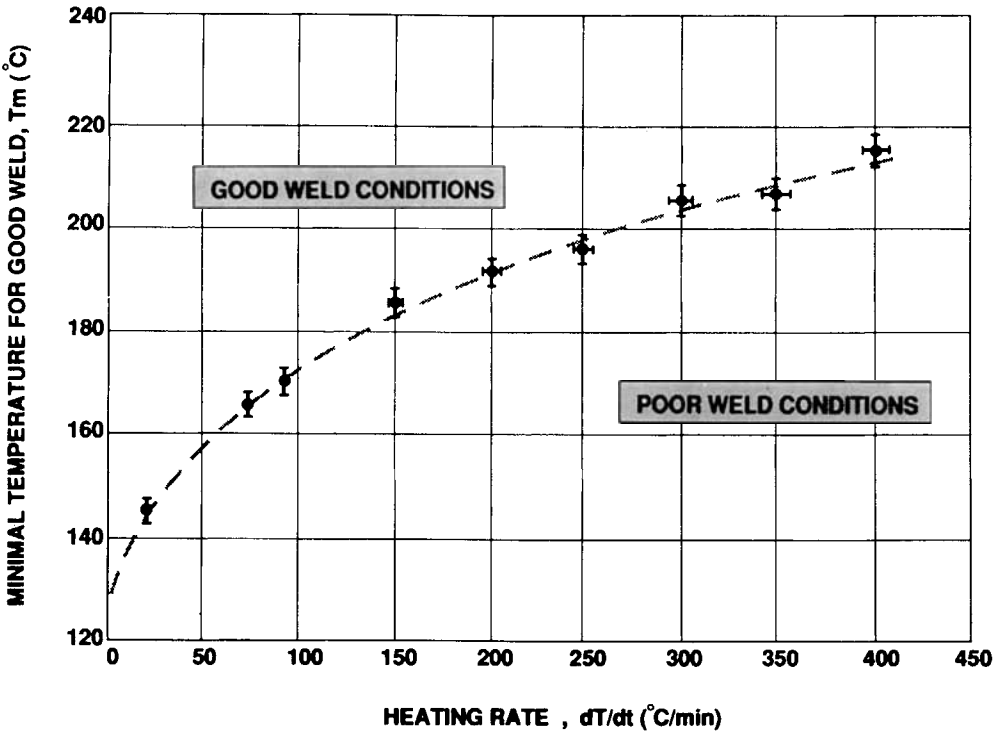

Fig. 6. Experimental welding behavior of polyethylene sheets: heating rate dependence of minimum good weld temperature: The dashed line represents the function $T_m = 4.3\,(dT/dt)^{1/2} + 401.4$ (where T_m is expressed in K), obtained by regression, with a correlation coefficient of 0.994.

with a power law. A good correlation is obtained for an exponent of 0.5 ± 0.1. In particular, with a value of 0.5, the expression obtained (correlation coefficient = 0.994) is in the form

$$T_m = 4.3(dT/dt)^{1/2} + 401.4 \tag{2}$$

where T_m is expressed in K.

This relation shows that the greater the heating rate [i.e., the shorter the time t_m defined above (see Fig. 2)] the higher the minimum temperature needed for an optimum weld. The extrapolation of eq. (2) at zero heating rate dT/dt leads to a value of T_m near 128°C. This value is close to the melting temperature of the polyethylene studied (135°C). Therefore, the temperature value at zero rate from eq. (2) represents the limit temperature T_0, below which optimum welding of specimens can never be achieved, even for infinite welding times (i.e., $dT/dt = 0$).

Figure 6 reveals two theoretical thermal areas bounded by the curve $T_m = f(dT/dt)$. Below this curve, the thermal conditions ($[dT/dt]$; T) are such that the temperature T_s reached is always lower than T_m, whatever the rate dT/dt. Optimum welding conditions are therefore never reached in this area. Above the curve, the thermal conditions ($[dT/dt]$; T) are such that the temperature T_s reached is always greater than T_m, whatever the heating rate. Therefore, in this area the weld is always good according to the above-defined criterion.

Optimal Conditions for Fusion Welding Process. Theoretical Approach

There have been numerous studies about mutual adhesion of polymeric materials. It can be reasonably assumed that adhesion results from the superposition of two phenomena: first, "wetting" which involves the surface tensions of the two surfaces in contact (this phenomenon predominates at low welding temperatures close to the polymer melting point); second, interdiffusion of macromolecular chains of the two surfaces in contact which predominates at fairly high temperatures and welding times.[5-10] The microscopic approach to the phenomenon[11-15] is based mainly on a model of reptation of interpenetrating macromolecules moving in virtual "tubes" (which represent topological constraints for an isolated chain) proposed by De Gennes.[12]

The phenomena of adhesion by molecular interdiffusion are governed mainly by temperature and time. According to De Gennes et al.,[10,11,15,16] and in the case of amorphous polymers, the cohesion of welded joint can be represented by the energy of separation G_{IC}. This is either related to the density of entanglements created at the interface while maintaining the two surfaces in contact at a given temperature, or to the depth of chain interpenetration at the end of the welding period. Whatever the approach used, the energy of separation G_{IC} can be expressed as a function of the time of contact at a given temperature:

$$\frac{G_{IC}(t)}{G_{IC}(\infty)} = f\left[\frac{t}{t_\infty}\right] \tag{3}$$

where $G_{IC}(\infty)$ is equal to the maximum energy of separation obtained for a time t_∞, beyond which it no longer varies. Jud et al.[17] have shown that, for PMMA in particular, a power law can be defined experimentally between G and t, in the following form:

$$\frac{G_{IC}}{G_{IC}(\infty)} \sim \left[\frac{t}{t_\infty}\right]^{1/2} \tag{4}$$

Moreover, the welding time at a given temperature, t, can be related to the average curvilinear displacement of chains $\langle l^2 \rangle$ and to their diffusion coefficient in the "tubes," D_T, as follows:

$$\langle l^2 \rangle = 2 \cdot D_T \cdot t \tag{5}$$

a relation similar to that proposed by Einstein.

Equation (3) can therefore also be written

$$\frac{G_{IC}(t)}{G_{IC}(\infty)} = f\left[\frac{\langle l^2 \rangle}{\langle l_\infty^2 \rangle}\right] \tag{6}$$

According to the hypothesis of adhesion of surfaces in contact by molecular interdiffusion, one can imagine that, for amorphous polymers, peeling is based mainly on the reverse mechanism of macromolecules disentanglement.[8,10,18-21] We assume that this holds for polyethylene (semicrystalline), if low loads are applied and if the temperature is close to the softening point of the polymer (thus the macromolecular chains have a greater mobility). According to the interdiffusion theory, a perfect weld results in the "physical" disappearance of the interface. In this case, the molecules are deeply entangled and the energy of separation is equal to the cohesion energy of the material. The strength of the assembly under a given load therefore depends on the point of least resistance in one or other of the films. Despite the viscoelastic behavior of PE and its semicrystalline state at the temperature of the peel test, it can reasonably be assumed, by comparison with previous arguments, that the energy G required for peeling is related to the welding time by a relation similar to eq. (6):

$$\frac{G(t)}{G(\infty)} = f\left[\frac{\langle l^2 \rangle}{\langle l_\infty^2 \rangle}\right] \tag{7}$$

We have applied these theoretical concepts to our test methodology to link mathematically the thermal and mechanical parameters leading to the optimum weld quality. The previously defined criterion of a "good weld" must lead to an energy of separation G equal to or greater than G_m. According to eq. (7), this value G_m is reached for a value of $\langle l^2 \rangle$ equal to $\langle l_m^2 \rangle$. Consequently, the welding time at a given temperature, which gives the value G_m, is linked to $\langle l_m^2 \rangle$ by a relation similar to eq. (5):

$$\langle l_m^2 \rangle = 2 \cdot D_T \cdot t_m \tag{8}$$

This analysis corresponds to a welding process at constant temperature. For the present study, we propose the calculation given in the Appendix, which deals with welding under dynamic thermal conditions. With the calculation, the parameter D_T can be expressed as a function of the variables dT/dt and T directly available through experimentation. Assuming that D_T depends on temperature, according to a relation described by eq. (12) (see the Appendix), and using the equivalent temperature concept introduced by Ozawa,[22] eq. (16) is obtained. It gives the correlation between the thermal conditions imposed during welding and the mechanical quality of the weld between the two PE specimens. The calculation developed in the Appendix does not take account of the polydispersity of the resin studied. It has been assumed that it behaves like a monodispersed polymeric material characterized by the parameter N in eq. (11) of the Appendix. The parameters D_1 and $\langle l_m^2 \rangle$ used in the Appendix are therefore average quantities, characteristic of the material. Equation (A16) (Appendix) confirms the experimental behavior regarding the variations of T_m vs. dT/dt (Fig. 6). According to the above hypothesis, welding thermal conditions located on the curve $T_m = f(dT/dt)$ correspond to values of $\langle l^2 \rangle$, which are all the same and equal to $\langle l_m^2 \rangle$. Consequently, as dT/dt increases T_m must also rise so as to hold $\langle l_m^2 \rangle$ constant. This theoretical approach to fusion welding behavior involves two diffusion parameters, $E^\ddagger$ and $4D_1/\langle l_m^2 \rangle$.

Graphical Determination of the Diffusion Parameters

The two parameters $E^\ddagger$ and $4D_1/\langle l_m^2 \rangle$ in eq. (16) have been determined from the plot of the regression straight line, whose equation [(18)] is given in the Appendix:

$$\log\left[\frac{d(T_m^2)}{2 \cdot d(dT/dt)}\right] = \log\frac{\langle l_m^2 \rangle}{4D_1} + \frac{E^\ddagger}{RT_m}$$

and using an empirical relation between T_m and dT/dt in the form of eq. (2):

$$T_m = 4.3(dT/dt)^{1/2} + 401.4$$

The plot corresponding to eq. (18) is shown in Figure 7. The broken line indicates the most probable straight line. It was obtained with a correlation coefficient of 0.987. Its equation has the following form:

$$\log\left[\frac{T_m \cdot dT_m}{d(dT/dt)}\right] = 3945 \cdot T_m^{-1} - 4.13 \tag{9}$$

The slope of the straight line is proportional to the apparent diffusion activation energy, and the extrapolation for zero—T_m^{-1} gives the value of the coefficient $\langle l_m^2 \rangle / 4D_1$ (see the Appendix).

Numerical Simulation of Fusion Welding Behavior of Polyethylene

A correlation between the experimental behavior and the theoretical one modelled by eq. (16) (Appendix) has been researched to simulate the fusion welding behavior of the polyethylene under study.

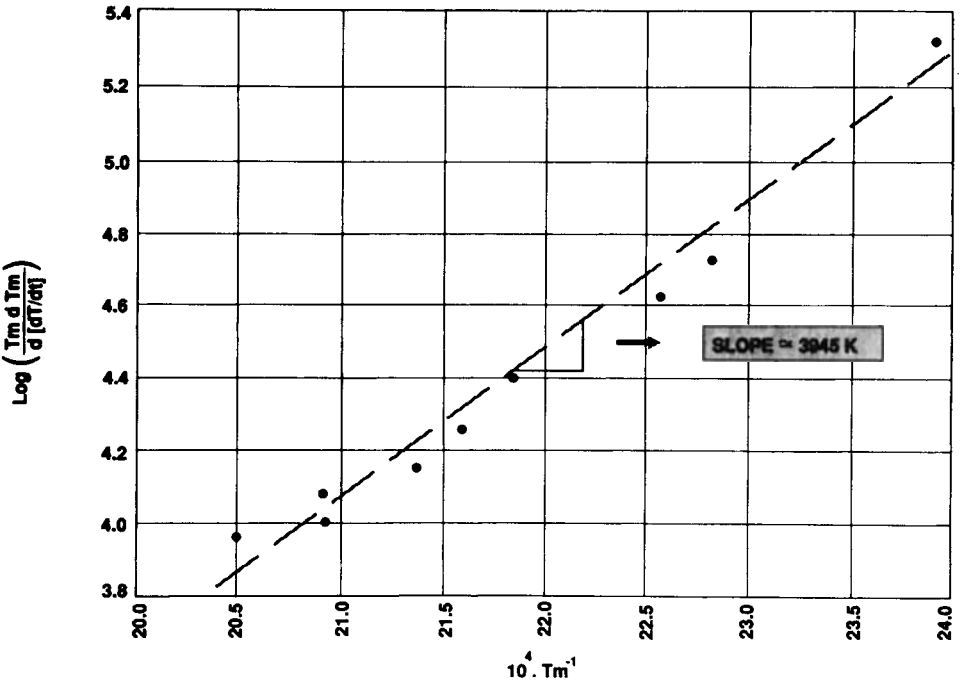

Fig. 7. Graphical determination of the diffusion parameters: the dashes represent the regression straight line corresponding to the function $\log[T_m\, d(T_m)/d(dT_m/dt)] = 3945T_m^{-1} - 4.13$, where T_m is expressed in K (correlation coefficient around 0.987). The slope of the line is proportional to the apparent diffusion activation energy $E^\ddagger$ and the constant value is representative of the coefficient $\langle l_m^2 \rangle / 4D_1$.

For this purpose, the two diffusion parameters leading to the numerical law closest to the experimental results have been calculated by the least squares method, using eq. (16)

$$\frac{\langle l_m^2 \rangle}{4D_1} \frac{dT}{dt} = \int_{T_0}^{T_m} T \cdot \exp\left(\frac{-E^\ddagger}{RT}\right) \cdot dT$$

Equation (16) was computed step by step from experimental thermal data ($[dT/dt]$; T_m) and by allowing the diffusion parameters, $E^\ddagger$ and $\langle l_m^2 \rangle / 4D_1$, to vary within a range of variations defined from the literature. An additional condition was imposed on the lower limit T_0 at very low heating rates. This limit was set at 135°C (temperature of the melting peak of the thermogram in differential scanning calorimetry) for a zero-heating rate (i.e., infinite heating time).

Comparison between Graphical Method and Numerical Simulation

Table I gives the results obtained for the diffusion parameters using either graphical method or numerical simulation. As a comparison, an experimental

TABLE I
Comparison between the Graphical Method and the Numerical Simulation[a]

	Graphical determination	Numerical determination	Viscosity measurement
$E^{\ddagger}$ (kJ/mol)	32.8	40.0	30
$\langle l_m^2 \rangle / 4D_1$ (s K)	0.02	0.13	—

[a] Values obtained for the diffusion parameters.

value of the viscosity activation energy at zero-shear gradient is also given for the same material.

It can be seen that the value of $E^{\ddagger}$ determined graphically, i.e., 32.8 kJ/mol, is quite close to the viscosity activation energy, 30 kJ/mol. On the other hand, the value of $E^{\ddagger}$ calculated with the simulation model, i.e., around 40 kJ/mol, is higher than the one determined graphically. For the parameter $\langle l_m^2 \rangle / 4D_1$, the tendency is the same as above. The value obtained from graphical determination is about six times lower than the one calculated with simulation.

The deviations observed can have three major causes. The first is due to the empirical nature of eq. (2) defined from the experimental data. Indeed, the choice of a logarithmic relation between T_m and dT/dt, also valid, leads to a

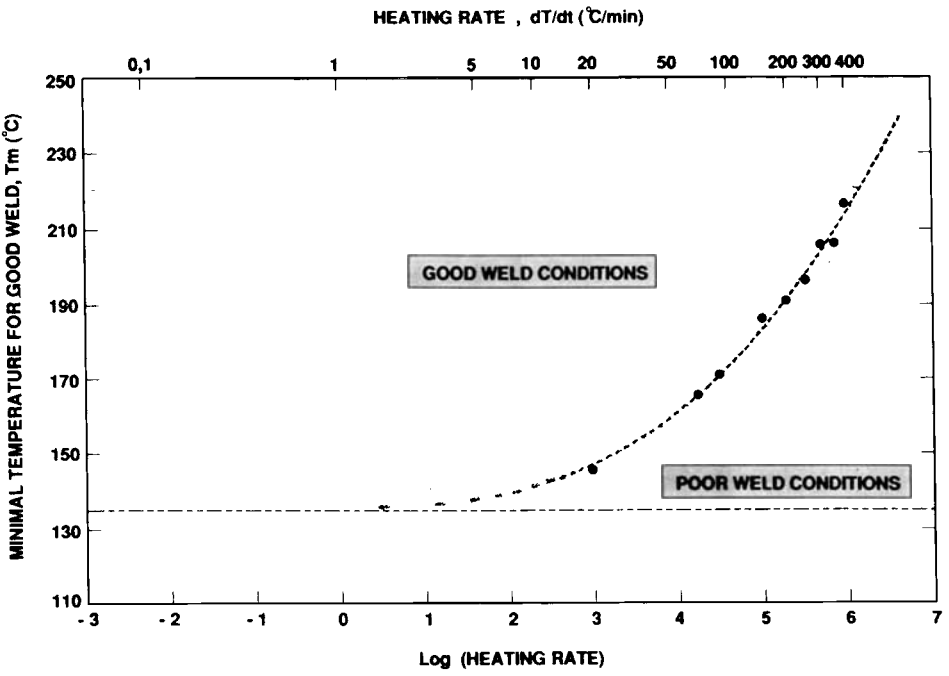

Fig. 8. Numerical simulation of the welding behavior of polyethylene specimens: Minimum good weld temperature T_m vs. Neperian logarithm of heating rate dT/dt: (●) Experimental points; (superposed broken line) numerical model; (horizontal dashes) lower limit temperature T_0.

value of $E^{\ddagger}$ of about 69 kJ/mol, which is considerably higher than the viscosity energy. The second cause is related to the inaccuracy in the determination of the viscosity activation energy at zero-shear rate, given the effects of polydispersity of the material. The third source of error may be the result of experimental deviation concerning the two thermal data ($[dT/dt]$; T_m) injected in the model. The apparent diffusion activation energy in eq. (16) (Appendix) can therefore easily be assimilated to the viscosity activation energy for a zero-shear rate. In addition, the values found in the literature show the mediocre accuracy in the determination of diffusion energy $E^{\ddagger}$.

The broken line in Figure 8 shows the result of the numerical integration of eq. (16) superposed on the experimental data, for heating rates between 0 and 400°C/min. The value of the variance (difference between the experimental points and the theoretical curve) indicates that the mean error for the heating rates is less than 17°C/min for the entire curve. Consequently, eq. (16) provides a good model of the experimental behavior of this resin when welded to itself in the range of rates studied. Our limited data is in accord with the predictions of macromolecular interdiffusion theory. Equation (16) therefore enables us to predict, for each heating rate dT/dt, the corresponding minimum temperature T_m to be reached in order to obtain a satisfactory weld quality [upper part of graph $T_m = f(\log dT/dt)$].

CONCLUSION

The methodology described here is well suited to the study of physicochemical phenomena occurring at the interface of two polyethylene parts assembled by fusion. The experimental results have shown that the bonding of the two surfaces is probably governed by a mechanism of macromolecular interdiffusion. The fusion welding behavior of this resin can thus be simulated by a mathematical model based on this theory and which brings into play two parameters characteristic of the diffusion of macromolecular chains. The method can be used both to compare the fusion welding behavior of different PE resins and to establish a correlation between the diffusion parameters of the model and the average molecular weights of these resins.

APPENDIX: RELATION BETWEEN OPTIMUM PARAMETERS FOR A "GOOD WELD"

From eq. (8),

$$\langle l_m^2 \rangle = 2 \cdot D_T \cdot t_m \tag{10}$$

it is possible to relate $\langle l_m^2 \rangle$ to the thermal parameters dT/dt and T_m leading to an "optimal" weld, by expressing D_T and t_m by means of these variables. In particular, the diffusion coefficient D_T can be expressed as follows[23,24]:

$$D_T = \frac{k \cdot T \cdot N_e}{3\xi_0} \cdot N^{-2} \tag{11}$$

where k is the Boltzmann constant (J K^{-1}), T the temperature (K), N_e the number of monomer units between entanglements, N the number of monomer units of the diffusion chain, and ξ_0 the coefficient of friction of a monomer unit (N s cm^{-1}).

According to a postulated relation of proportionality between ξ_0 and the viscosity of the melt at zero-shear rate, eq. (11) becomes

$$D_T = D_1 \cdot T \cdot \exp(-E^\ddagger/RT) \tag{12}$$

where $E^\ddagger$ represents the apparent activation energy of diffusion in the "tube," similar to the viscosity activation energy. A coefficient of diffusion averaged for the entire welding cycle can be introduced:

$$D_T = \frac{1}{t_m} \cdot \int_0^{t_m} D(T) \cdot dt = D_{T_e} \tag{13}$$

Equation (13) also introduces the notion of equivalent temperature T_e proposed by Ozawa.

From the run of the profile of the thermal welding cycles (see Fig. 2) it is convenient to consider this diffusion coefficient averaged over the range $[T_0, T_m]$:

$$D_T = (T_m - T_0)^{-1} \cdot \int_{T_0}^{T_m} D(T) \cdot dT \tag{14}$$

As for the minimum time for a "good weld," t_m, it can be expressed in the form

$$t_m = 2(T_m - T_0) \cdot (dT/dt)^{-1} \tag{15}$$

By including eqs. (14) and (15) in eq. (10), it becomes

$$\frac{\langle l_m^2 \rangle}{4D_1} \frac{dT}{dt} = \int_{T_0}^{T_m} T \cdot \exp\left(\frac{-E^\ddagger}{RT}\right) \cdot dT \tag{16}$$

Equation (16) links the thermal and mechanical conditions representative of an optimum weld quality between the two polyethylene specimens.

It is thus possible to obtain a formula suitable for the experimental results $T_m = f(dT/dt)$ and then to obtain the diffusion parameters. By differentiating eq. (16) with respect to T_m, and taking the reverse of the form obtained, it follows that

$$\frac{T_m \, d(T_m)}{d(dT/dt)} = \frac{\langle l_m^2 \rangle}{4D_1} \cdot \exp\left(\frac{E^\ddagger}{RT_m}\right) \tag{17}$$

The transformation of eq. (17) into the logarithmic form leads to

$$\log\left[\frac{d(T_m^2)}{2d(dT/dt)}\right] = \log\frac{\langle l_m^2 \rangle}{4D_1} + \frac{E^\ddagger}{R} \cdot T_m^{-1} \tag{18}$$

Equation (18) enables one to deduce the value of the diffusion parameters $E^\ddagger$ and $\langle l_m^2 \rangle / 4D_1$ from the experimental curve $T_m = f(dT/dt)$ (see Fig. 7).

References

1. M. D. Ellul and A. N. Gent, *J. Polym. Sci., Polym. Phys. Ed.*, **22**, 1953 (1984).
2. S. Yamakawa, *Polym. Eng. Sci.*, **16**, 411 (1976).
3. D. H. Kaeble, *Trans. Soc. Rheol.*, **9**, 135 (1965).
4. K. Kendall, *J. Adhesion*, **5**, 179 (1973).
5. A. N. Gent and J. Schultz, *J. Adhesion*, **3**, 281 (1972).
6. L. Lavielle and J. Schultz, *Mater. Tech.*, 215 (1984).

7. J. Schultz and A. Carré, *Inf. Chim.*, **232**, 101 (1982).
8. S. S. Voyutskii and V. L. Pakula, *Rubber Chem. Technol.*, **37**, 1153 (1964).
9. L. Bothe and G. Rehage, *Rubber Chem. Technol.*, **55**, 1308 (1982).
10. K. Jud and H. H. Kausch, *Polym. Bull.*, **1**, 697 (1979).
11. P. G. De Gennes and L. Leger, *Ann. Rev. Phys. Chem.*, **33**, 49 (1982).
12. P. G. De Gennes, *J. Chem. Phys.*, **55**(2), 572 (1979).
13. J. Klein and B. J. Briscoe, *Proc. R. Soc. London A*, **365**, 53 (1979).
14. P. G. De Gennes, *C.R. Acad. Sci. Paris, Sér. B*, **291**(9), 219 (1980).
15. R. P. Wool and K. M. O'Connor, *J. Appl. Phys.*, **52**, 5953 (1981).
16. S. Prager and M. Tirrel, *J. Chem. Phys.*, **75**(10), 5194 (1981).
17. K. Jud, H. H. Kausch, and J. G. Williams, *J. Mater. Sci.*, **16**, 204 (1981).
18. H. H. Kausch and K. Jud, *I.U.P.A.C., 26th Int. Symp. on Macromolecules*, Mainz, Sep. 1979, p. 1426.
19. A. N. Gent and R. H. Tobias, *J. Polym. Sci., Polym. Phys. Ed.*, **22**, 1483 (1984).
20. S. S. Voyutskii and Y. L. Margolina, *Rubber Chem. Technol.*, **30**, 531 (1957).
21. H. H. Kausch, 4th International Conference on Deformation Yield and Fracture of Polymers, Cambridge, Apr. 1979.
22. T. Ozawa, *Thermal Analysis: Comparative Studies on Materials*, H. Kambe and P. D. Garn, Eds., Halsted, New York, 1974, p. 155.
23. C. R. Bartels, B. Crist, and W. W. Graessley, *Macromolecules*, **17**, 2702 (1984).
24. G. Fleischer, *Colloid Polym. Sci.*, **265**, 89 (1987).

Received April 20, 1988
Accepted August 10, 1988